Viscoelastic Properties and Film Morphology of Heterogeneous Styrene–Butadiene Latexes

ROGER HAGEN,[1,*] LENNART SALMÉN,[1] OLA KARLSSON,[2] and BENGT WESSLÉN[2]

[1]STFI, (Swedish Pulp and Paper Research Institute), Box 5604, S-114 86 Stockholm, and [2]Lund Institute of Technology, Chemical Center, Department of Chemical Engineering, Box 124, S-221 00 Lund, Sweden

SYNOPSIS

Heterogeneous carboxylated styrene–butadiene (S/Bu) latexes were prepared by a two-stage emulsion polymerization process, using three PS seeds with different molecular weights. The second-stage polymer was a copolymer with a fixed S/Bu ratio of 1 : 1 and a methacrylic acid (MAA) content of either 1 or 10 wt %. Morphological studies by transmission electron microscopy (TEM) as well as studies of the viscoelastic properties by mechanical spectroscopy have been performed on films prepared from the latexes. The studies showed that the glass transition temperature, T_g, of the second-stage polymer was considerably affected by copolymerization with MAA. An increase in the MAA content in the second-stage polymer increased the T_g of this phase significantly. Addition of DVB as a crosslinking agent in the preparation of the PS seed phase substantially increased the rubbery moduli of the films, whereas the glass transition temperature of the second-stage polymer was unaffected. On the other hand, the presence of a chain transfer agent reduced the glass transition of the second-stage copolymer containing 1 wt % MAA dramatically, whereas the rubbery modulus was unaffected. When the MAA content was increased to 10 wt % the influence of the MAA monomer had a dominating effect on T_g. Latexes containing 10 wt % MAA had T_g values close to each other, regardless of chain transfer agent present in the second-stage polymerization. It was found that the morphology of the latex particles influenced the rubbery modulus of the films. The presence of irregularly shaped seed particles in samples prepared from a crosslinked PS seed had a considerable reinforcing effect on the films, whereas spherical seed particles originating from core–shell particles had a less reinforcing effect. © 1996 John Wiley & Sons, Inc.

INTRODUCTION

Styrene–butadiene (S/Bu) latex is one of the most common latex systems for binder applications in paper coatings. Copolymer latexes are generally prepared by a single-stage emulsion polymerization. The ratio of styrene to butadiene in the copolymer is a key parameter for the film-forming properties and for the final viscoelastic and mechanical properties of the latex film. For the copolymer, the hardness, the brittleness, and the glass transition temperature, T_g, increase with increasing styrene content, whereas the flexibility increases with increasing butadiene content. Styrene–butadiene binders for the paper and board industry generally contain between 30 and 50% copolymerized butadiene by weight.[1] The surface of the latex particles is often modified by incorporating small amounts (0–10%) of vinyl acids, e.g., acrylic acid or methacrylic acid,[2] to increase adhesion between the latex particles and the substrate or the pigment, to enhance curing reactions in the latex films, and to increase the colloidal stability of the latex particles.[3,4]

A combination of low film-forming temperature and high modulus at ambient temperatures is difficult to obtain with conventional S/Bu copolymers latexes. However, by using heterogeneous latexes as binders for paper coatings this combination of properties might be attainable. Heterogeneous latex particles having different particle

* To whom correspondence should be addressed.

Journal of Applied Polymer Science, Vol. 62, 1067–1078 (1996)
 CCC 0021-8995/96/071067-12

morphologies can be prepared by multistage emulsion polymerization processes. If a different monomer is used in the second stage in a seeded polymerization, a phase separation occurs and many different types of heterogeneous morphologies are formed.[5-12] For example, the properties of a film prepared from a core–shell latex may be characterized by a combination of a low film-forming temperature due to a low glass transition temperature of the soft phase and a high stiffness due to a high T_g of the seed particle polymer. Particle morphology and grafting between the phases are strongly influenced by the crosslink density of the seed latex.[13] The seed particles may be crosslinked by the incorporation of an external crosslinking agent such as divinyl benzene.[14]

In this work, heterogeneous styrene–butadiene latexes have been prepared by a two-stage emulsion polymerization, using different types of styrene seed latex (the core) and using a fixed Bu/S ratio and different amounts of methacrylic acid (MAA) as a functional monomer[15] in the second phase copolymer (the shell). The morphologies of particles and films have been studied by transmission electron microscopy (TEM), and the viscoelastic properties of the latex films have been characterized by mechanical spectroscopy. In a separate article,[16] the polymerization kinetics and more details concerning the particle morphologies are discussed.

EXPERIMENTAL

Materials

Styrene (S) (Merck, pro analysi), divinyl benzene (DVB) (Merck, pro analysi) and methacrylic acid (MAA) (Merck, pro analysi) were purified by passing through a column filled with aluminium oxide (Merck, active base). The purified monomers were kept at 4°C before use. Butadiene (Bu) (Air Liquide, min 99.5%) was purified by passing through a column filled with aluminium oxide (Merck, active base) and freshly distilled before use. Distilled and deionized water was used. All other chemicals were of analytical grade and were used as supplied.

Latex Synthesis

Preparation of Seed Latexes

Three different types of styrene seed latex were prepared in a 2-L calorimetric reactor (ChemiSens RM-2L) at 70°C using potassium persulfate (KPS) as the initiator and sodium dodecyl sulfate (SDS) as the emulsifier.

Seed A was an unmodified PS latex. In seed B, the molecular weight of the seed latex polymer was lowered by the use of carbon tetrachloride (CCl_4) as a chain transfer agent. The CCl_4 was charged together with the monomer at a ratio of 5 : 100 based on the monomer. In seed C, 90% of the total monomer was charged prior to the polymerization. The last 10% of monomer charged consisted of a mixture of divinyl benzene (DVB) and styrene at a DVB : S ratio of 4 : 100. The DVB/S addition was a semibatch operation at starved conditions near the end of the polymerization, in order to achieve crosslinked particle shells having residual double bonds. Detailed descriptions of the polymerizations are given elsewhere.[16]

Prior to the second polymerization stage, the seed latexes were thoroughly dialyzed at ambient temperature in order to remove inorganic ingredients, monomers, and in some cases chain transfer agents. A membrane with MWCO: 6–8000 (Spectra/Por™, Spectrum Medical Industries, Inc, CAL, USA) was used with a SDS solution (1.5 g SDS L^{-1} H_2O) prepared from distilled and deionized water. The SDS solution was changed daily during two weeks. After this time, the solids contents of the latexes were determined.

Second-Stage Polymerization

The second-stage polymerization was performed at 80°C as a seeded batch process using a 250 mL high-pressure calorimetric reactor (ChemiSens RM-2S). The heat of polymerization was measured and monitored on line and used to calculate the conversion. The ratio of the seed to the stage 2 monomer was 1 : 1 in all the polymerizations. The second stage polymer was poly(butadiene-*co*-styrene-*co*-methacrylic acid) (Bu/S/MAA) using a fixed Bu/S ratio of 1 : 1, and the MAA content was either 1 or 10 wt %. The initiator concentration was 1×10^{-3} mol/L and no additional emulsifier was used.

Two latex samples having the same overall composition as the second-stage polymer were prepared as references. These polymerizations were performed as batch polymerizations under the same conditions as the second-stage polymerizations. The compositions of both the second-stage latex and the reference latex are given in Table I. Further details of the polymerizations are given elsewhere.[16]

Experimental Methods

Film Preparation

Films were prepared by applying latex with an applicator bar onto clean glass plates. The latex films

Table I Composition of Materials

Latex	A1	A10	B1	B10	C1	C10	R1	R10
Seed	A[a]	A[a]	B[b]	B[b]	C[c]	C[c]	—	—
MAA (wt %)	1	10	1	10	1	10	1	10
S (wt %)	49	45	49	45	49	45	48	44
Bu (wt %)	50	45	50	45	50	45	51	46

[a] Seed A is a batch polymerized PS latex without any modification.
[b] Seed B is a batch polymerized PS latex with CCl_4 added.
[c] Seed C is a semibatch polymerized PS latex with DVB added late in the polymerization.

were then dried at 50°C and 8% relative humidity. Samples for TEM, DSC, and DMA analysis were cut from the same film pieces.

Differential Scanning Calorimetry (DSC)

Polymer films were analyzed with a Mettler DSC 30 instrument equipped with a low-temperature cell. The film samples were first heated to 130°C at 15°C min^{-1}. After 5 min at 130°C, the samples were cooled to −150°C at a rate of 15°C min^{-1}, and finally reheated to 300° at a rate of 10°C min^{-1}. The last run was used to determine the T_g.

Dynamic Mechanical Analysis (DMA)

Mechanical spectroscopy was performed in tension using a Perkin–Elmer DMA-7 with a stainless steel measuring system. Helium was used as a purge gas at 40 cm^3 min^{-1}. Liquid nitrogen was used as the furnace coolant, allowing for temperature scans from −70 to 80°C for most of the specimens. A heating rate of 2°C min^{-1} and a frequency of 1 Hz were chosen during the temperature scans. A temperature calibration was conducted using the melting points of water (0.0°C) and indium (156.6°C) at the same heating rate as that at which the measurements were performed, to minimize errors due to thermal lag. The applied stress was chosen to ensure that the experiments were within the linear viscoelastic region. Specimens were 10 mm in length and 2 mm in width, with a thickness in most cases of approximately 0.2 mm. Smaller samples were used for latexes with poor film-forming properties.

Transmission Electron Microscopy (TEM)

The morphologies of the latex samples were examined with a JEOL 100 U transmission electron microscope. In order to avoid distortion of the latex particles during drying, osmium tetroxide (OsO_4) staining was done in the liquid phase.[17] Thin latex film pieces were cut using a razor blade. These small film pieces were stained with OsO_4 vapour and imbedded in Epon 812. Sections, 60 nm thick, of the imbedded films were cut using a LKB Ultatome V for examination in the microscope. In the TEM micrographs, the polybutadiene (PB)-containing phase appears as dark domains and the polystyrene (PS)-containing phase as bright domains. The average particle diameters were calculated from measurements on micrographs of OsO_4-stained latex particles.[17]

Gel Permeation Chromatography (GPC)

Gel permeation chromatography (GPC) of the seed latexes was performed on a chromatographic system (Waters Associates) equipped with a dual detector containing both RI and viscosity detectors (Viskotek, Model 250) and a LALLS detector (LDC-analytical, KMX-6). A series of three columns (Waters μ Styragel, 10^5, 10^4, 10^3 Å) was used at ambient temperature. The GPC columns were calibrated using six PS standards (Polymer Laboratories) with narrow molecular weight distributions. The tetrahydrofuran, THF, flow rate was set at 1.0 mL min^{-1}. All seed latexes were dissolved in THF and after 24 h the samples were filtered though a 0.2 μm filter, and 150 mL of the filtrate [0.003 mg mL^{-1} THF] was injected. The molecular weights presented are defined as the GPC peak value, M_{GPC}.

RESULTS

Particle Morphology

The particle morphologies found for latexes A1 and B1 are shown in the TEM micrographs given in Figure 1(a,c). The compositions of the latexes are given in Table I. The latex particles had similar hemispherical morphologies. A close look at the micrographs shows that the phase separation was more pronounced in latex B1, which was made from the seed with the lowest molecular weight (seed B). The

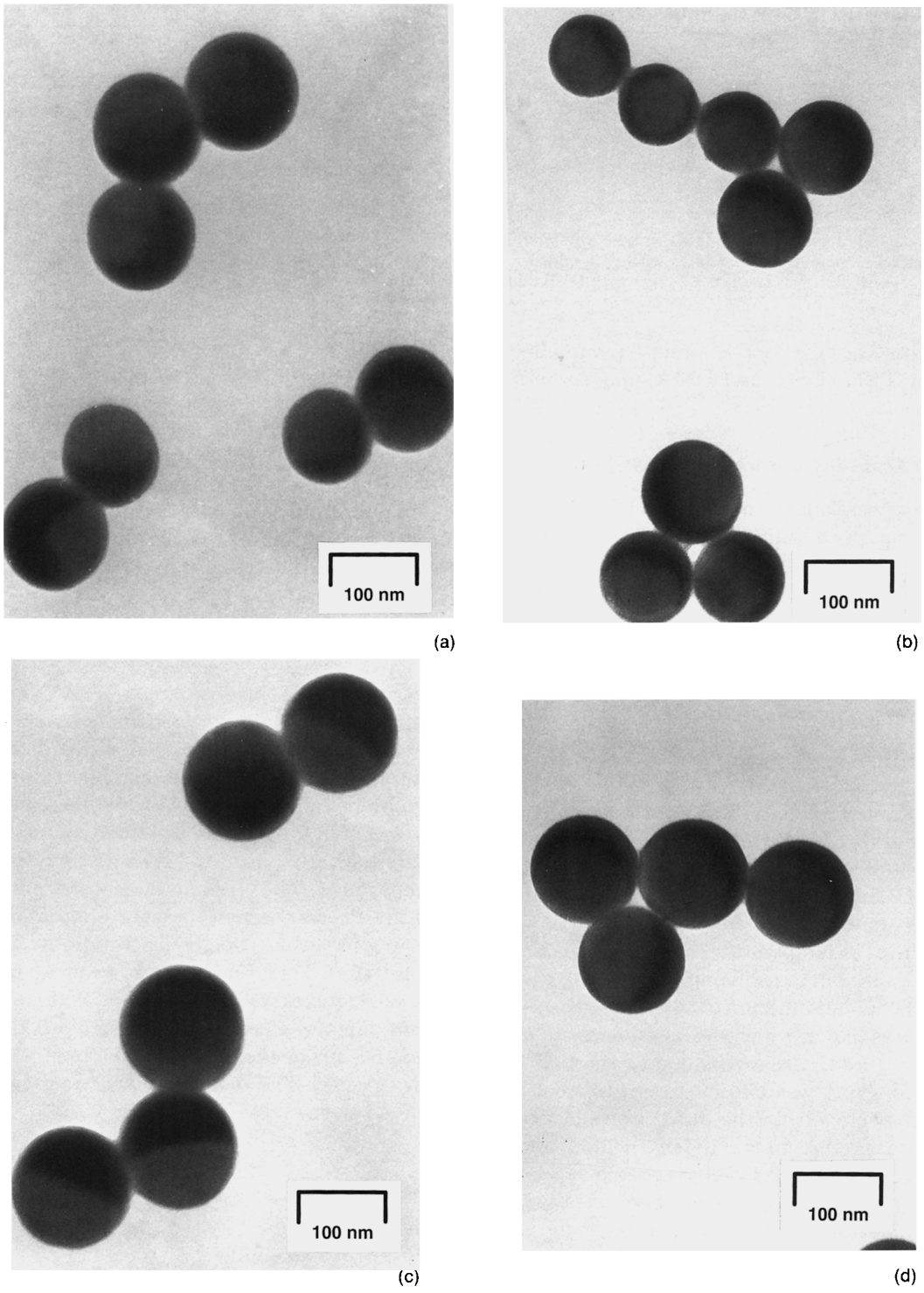

Figure 1 TEM micrographs of the particle morphology of latexes: (a) A1, (b) A10, (c) B1, (d) B10, (e) C1, (f) C10.

particles in latex B1 are composed of two half-spheres, in contrast to the acorn-like structures in latex A1. Figure 1(e) shows a micrograph of latex C1 that was made from the semibatch polymerized seed with a DVB-rich shell. These latex particles had a morphology that can be described as an oc-

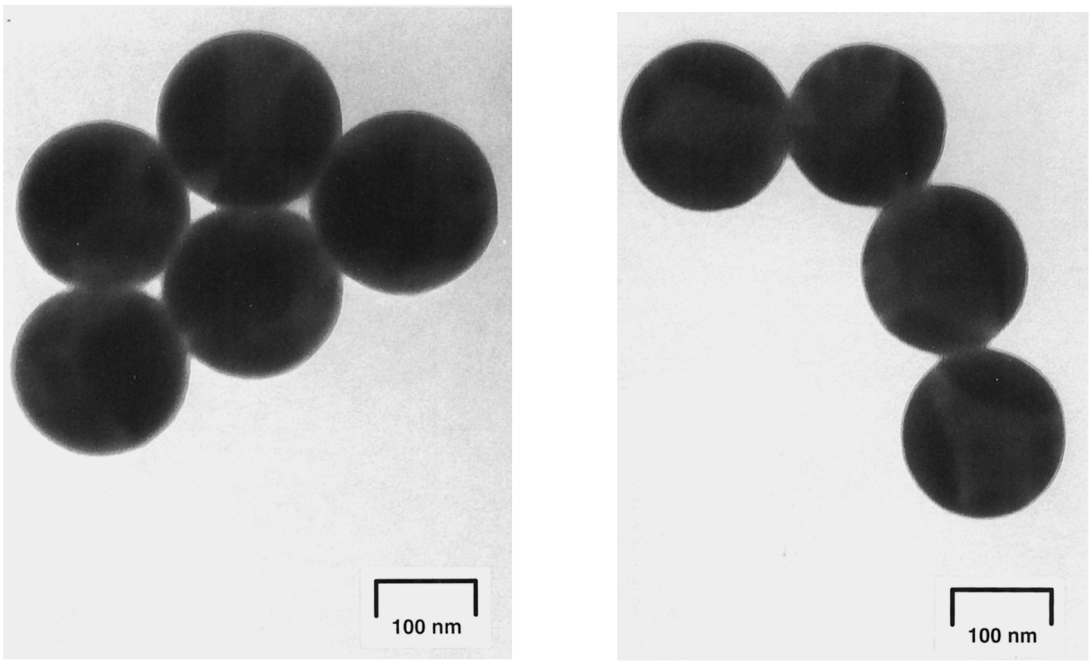

(e) (f)

Figure 1 (*Continued from the previous page*)

cluded simplified hemisphere (SHSOCC).[12,18] The different particles show several occlusions of different sizes of the second-phase polymer distributed in the seed polymer matrix. The morphological differences observed among latexes A1, B1, and C1 seem to depend on the seed molecular weight and on the internal particle viscosity during the second polymerization stage. The seed and latex particle diameters and the molecular weights of the seed particle polymers are summarized in Table II.

The particle morphologies in latexes A10 and B10 look similar, as is shown in Figure 1(b,d). Both latexes show close to core–shell morphologies, with the hydrophilic second-stage polymer almost completely surrounding the seed polymer particles. The particle morphology of latex C10, given in Figure 1(f), corresponds to an occluded hemispherical type similar to that of latex C1. The large second-stage polymer domain present in the particles has an appearance in latex C10 different from that in latex C1. In C10, which has the higher MAA content, the domain was located outside the original seed particle, trying to grasp it. In latex C1, the large domain seemed to be located close to the particle surface

Table II Latex Particle Sizes as Obtained by TEM and Corresponding Seed Molecular Weights

Latex	Seed Diameter (nm)	Particle Diameter (nm)	Seed MW (M_{GPC} 10^{-3})
A1	88	124	1300
A10	88	120	1300
B1	90	135	230
B10	90	119	230
C1	137	188	1350
			> 4000[a]
C10	137	179	1350
			> 4000[a]
R1	—	160	—
R10	—	100	—

[a] A polymer fraction above the exclusion limit of the column system.

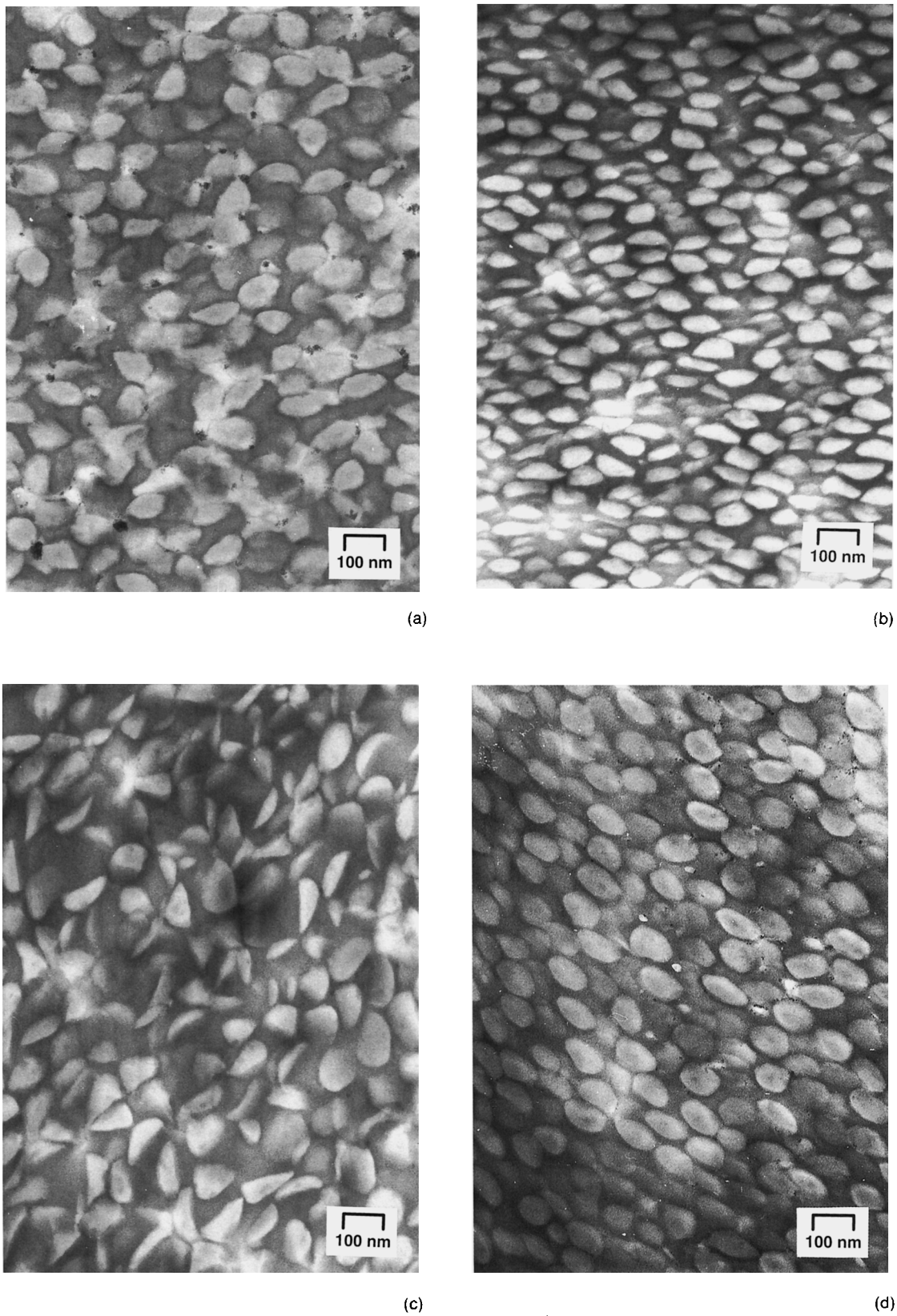

Figure 2 TEM micrographs of the film morphology of latexes: (a) A1, (b) A10, (c) B1, (d) B10, (e) C1, (f) C10.

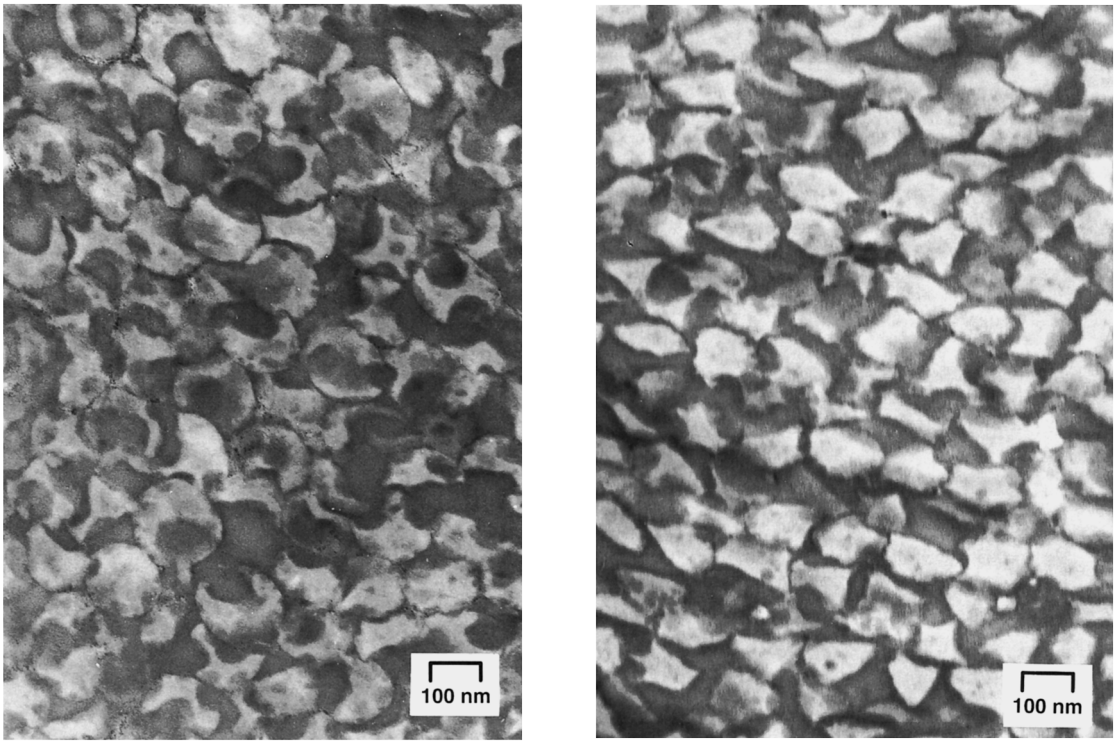

(e) (f)

Figure 2 (*Continued from the previous page*)

but still covered by the seed polymer. A similar morphological development when the hydrophilicity of the second-stage polymer was increased was reported in an earlier work.[12]

Visual Inspection of Latex Films

Films were made as described in the Experimental Section. The latexes prepared from the PS seed having a low molecular weight formed continuous films at both the 1 and 10% MAA levels (samples B1 and B10). The latex samples prepared from unmodified seed particles, i.e., samples A1 and A10, also formed continuous films. However, in sample A10, cracks appeared in the film when it was dried, giving small pieces of film of the order of one cm^2. High seed crosslinking and large seed particles resulted in poor film formation, as has previously been observed by O'Connor and Tsaur[14] for two-stage latex polymers based on butyl acrylate and styrene. Sample C10 formed 2–3 cm long rods and sample C1 millimeter-sized film fragments. The films obtained from both the reference latexes R1 and R10 were both soft, rubber-like, and tacky.

Film Morphology

TEM examination of OsO_4-stained films showed that seed latex particles could be seen as bright spherical domains in a dark matrix of the second-stage polymer. With regard to their morphologies, the six films can be divided into three main groups. The first group consists of latex films A1 and B1, shown in Figure 2(a) and (c). In both films, the smooth PS seed hemispheres of seed latex A and B, respectively, are distributed in a matrix of the second-stage polymer. The PS seed hemispheres seem to be clustered rather than evenly distributed in the film, forming a continuous network in the films through particle–particle contacts. The second group consists of latex films from C1 and C10, shown in Figure 2(e) and 2(f). In these films, the small occlusions of the second-stage polymer seen in the original latex particles can easily be observed. The hollow seed particle fragments from seed latex C form a continuous network throughout the films in a manner similar to that in the first group. The roughness of the residual seed latex particle surfaces may mean that the potential for particle–particle contacts is greater than in group one.

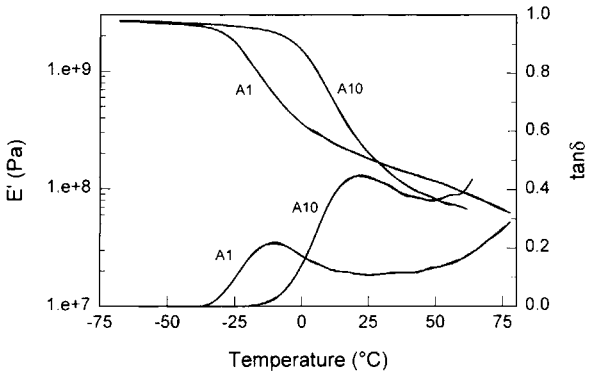

Figure 3 Storage modulus, E', and loss factor, tan δ, vs. temperature for films from samples A1 and A10.

The third group consists of the films from latexes A10 and B10, shown in Figure 2(b,d). In these two films, the residual seed latex particle fragments were evenly distributed in the second-stage polymer. As a consequence of the almost perfect core–shell morphology of the latex particles, the seed fragments found in these films were spherical, especially in the film from latex B10. In contrast to the films in group one, there were no contacts between the seed particle fragments in the films.

Dynamic Mechanical Properties

The dynamic mechanical behavior of films from latexes A1 and A10 is shown in Figure 3. The temperature region investigated encompasses the glass transition region of the second phase copolymer, and shows a peak in tan δ and a decrease in the storage tensile modulus, E'. An increase in the MAA content in phase 2 from 1 to 10% raised the glass transition temperature, T_g, as determined from the maximum in tan δ at 1 Hz, from −10 to 24°C. The shift in T_g may be explained by the higher content of MAA leading to more extensive hydrogen bonding.[19] PMAA has a T_g of 205°C, compared to −73°C for polybutadiene and 102°C for polystyrene, and the addition of MAA as a comonomer should thus increase the T_g of the copolymer.

The rubbery modulus was higher for latex A1 than for latex A10, presumably as a consequence of the interparticle contacts between the seed particles seen in sample A1. The less reinforcing effect of the seed particles in latex A10 was also manifested by the large peak value of the loss factor, tan δ_{max}. A similar phenomenon was suggested to be the explanation for the mechanical behavior of films prepared from heterogeneous styrene–butyl acrylate latexes by Cavaille et al.[20] A low glass transition temperature and a high modulus at temperatures above T_g are desired properties of the core–shell latexes.

In the region of the glass transition temperature of the polystyrene seed phase at approximately 100°C (DSC data), an increase in the loss factor and a decrease in the storage tensile modulus were recorded, as seen in Figure 3. Because of the softness of the latex films, it was difficult to perform dynamic tensile measurements due to subsequent creep at these temperatures.

Films prepared from latexes B1 and B10 showed larger differences in T_g between the samples containing 1 and 10% MAA, respectively, than the corresponding samples from latexes A1 and A10, as shown in Figure 4. Sample B1 had a T_g of −29°C, whereas sample B10 had a T_g of 18°C, i.e., the difference in T_g was 47°C. The drop in the modulus curve and the maximum in tan δ at T_g were more pronounced for sample B10 than for sample B1. The less reinforcing effect of the seed particles in latex B10 indicates that a larger fraction of the polymer was active in the softening process in sample B10 than in B1, which was also observed for the latexes prepared from the unmodified PS seed, i.e., samples A10 and A1.

Figure 5 shows DMA curves for latexes C1 and C10. These latexes were prepared from a PS seed crosslinked with DVB (seed latex C). Sample C1 showed a broad tan δ peak at approximately −13°C, corresponding to the main drop of the modulus curve. A peak in tan δ at approximately 25°C was also observed. The curve for sample C10 shows a tan δ peak at 13°C and a broadening of the curve at higher temperatures with a weak shoulder at approximately 25°C. These results indicate that there are two phases originating from the second-stage polymer. The DSC measurements revealed only a single glass transition, apparently connected to the

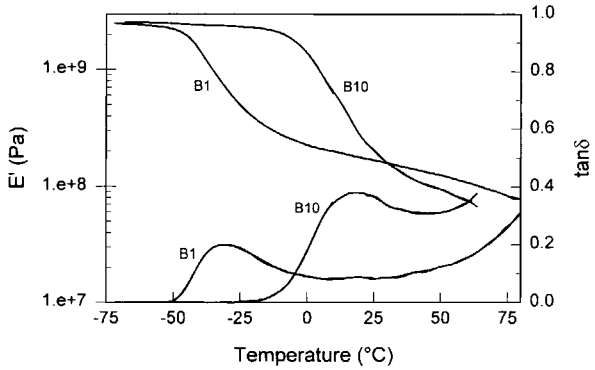

Figure 4 Storage modulus, E', and loss factor, tan δ, vs. temperature for films from samples B1 and B10.

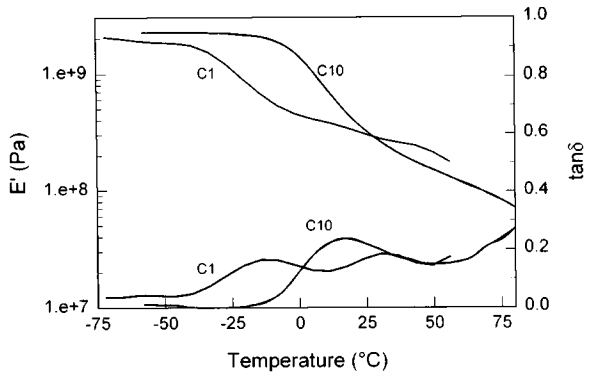

Figure 5 Storage modulus, E' and loss factor, tan δ, vs. temperature for films from samples C1 and C10.

low temperature transition in the DMA curves. The DSC transition occurs at −33 and 9°C for samples C1 and C10, respectively. However, dynamic mechanical testing is in general more sensitive than DSC for detecting glass transition temperatures, as has also been noted by others.[14,21,22]

For latexes prepared from the seed modified with DVB (C), the rubbery plateau modulus was higher for sample C1, containing 1% MAA, than for sample C10, containing 10% MAA. A similar difference was also observed for the latexes prepared from unmodified and CCl_4-modified seeds. Also in this case, the larger drop in modulus and the larger peak in tan δ noted for the samples containing 10% MAA in the second-stage polymer indicates that a larger fraction of the second-stage polymer is active in the relaxation process due to the less reinforcing effect. T_g data for the various latex films are summarized in Table III.

Figure 6 shows DMA curves of films prepared from batch polymerized copolymer latexes having S/Bu/MAA ratios similar to that of the second stage polymer in the two-phase latexes (R1 and R10). Two transitions are evident for both samples, with peaks in the tan δ curves at 0 and 23°C for R1 and at 6 and 24°C for R10, which indicates that two different polymer phases were present in the samples.

DISCUSSION

Large differences in morphology and viscoelastic properties were observed for the different heterogeneous latexes studied in this work. For example, the shapes and the packing of the latex particles in the films seem to have a large influence on the dynamic mechanical properties. The effects of the different types of polystyrene seed are obvious if DMA data for samples with the same monomer ratio in the second-stage polymerization are compared. Figure 7 shows a comparison of the dynamic mechanical properties of the latex films having a constant S/Bu/MAA ratio (50/49/1 wt %) but different types of styrene seed latex (samples A1, B1 and C1). A surprisingly low T_g value was obtained for the second-stage polymer in sample B1 based on PS-seed B, which had a reduced molecular weight caused by the addition of CCl_4 as a chain transfer agent. However, analysis of the seed by gas chromatography–mass spectrometry (purge and trap GC–MS) showed residual amounts of CCl_4, which had not been eliminated in or after the first polymerization step, even though the latex had been thoroughly dialyzed. As a consequence, the residual CCl_4 may have reacted with the monomers added in the second-stage reaction, and it seems probable that the molecular weight of the second-stage polymer was decreased by the presence of the chain transfer agent, which

Table III T_g of Latex Films

Latex	Soft Phase T_g (°C) (DMA, $(\tan\delta)_{max}$, 1 Hz)	Soft Phase T_g (°C) (DSC)	Hard Phase T_g (°C) (DSC)
A1	−10	−24	102
A10	24	7	103
B1	−29	−39	97
B10	18	6	101
C1	−13 and 25	−33	104
C10	13 and 25	9	102
R1	0 and 23	−9	—
R10	6 and 24	−4	—

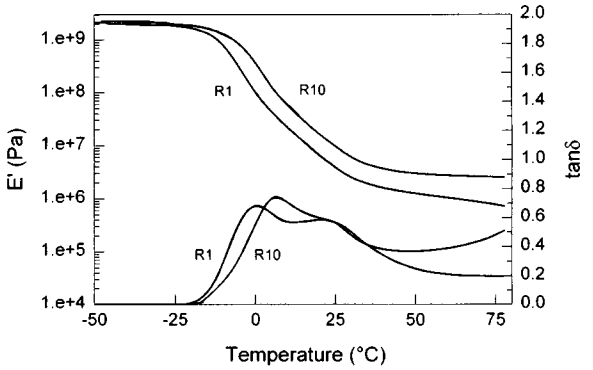

Figure 6 Storage modulus, E', and loss factor, tan δ, vs. temperature for films from batch polymerized copolymer latexes (samples R1 and R10).

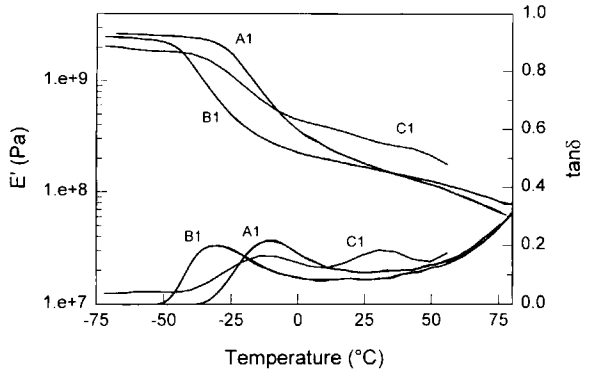

Figure 7 Storage modulus, E', and loss factor, tan δ, vs. temperature for films from samples A1, B1, and C1.

may contribute to the low T_g. The morphological differences between latex A1 and B1 particles can be explained by a low internal particle viscosity in latex B1 during the second-stage polymerization due to the lower molecular weight of both polymer phases in this latex.[16]

Samples A1 and C1 had similar T_gs as shown by the main drop of the modulus and the position of the peak in the tan δ curves. This means that the addition of DVB as a comonomer in the seed, to produce crosslinked seed particle surfaces and to introduce double bonds as possible grafting sites, had no influence on the major transition that gives the largest modulus reduction of the second polymer. However, the occurrence of a second transition at the higher temperature (25°C) could well be due to the low mobility of polymer chains bound to the surface of the seed particle by grafting reactions.

The difference between latexes A10 and B10 regarding particle morphology is much less noticeable than that between latexes A1 and B1. The hydrophilic properties of the second phase related to the MAA content seem to dominate over the effects of the molecular weight in the development of the morphology of the latex particles. The decrease in T_g observed in the case of the latex B1 film, presumably caused by a low molecular weight of the second-stage polymer, was absent in the case of the latex B10 film, even though the amount of residual chain transfer agent should be similar in this polymerization. Obviously, the higher MAA content in the second-stage polymer had an important effect on the film properties.

In the batch-polymerized reference latexes (R1 and R10), two transitions were observed in both samples when using DMA. The high temperature transition at approximately 25°C in R1 and R10 corresponds to the DMA transitions observed in the case of the latexes containing 10 wt % MAA in the second-stage copolymer. MAA has a larger effect on T_g for the S/Bu latexes than would be expected, if the T_g values of the second-stage copolymer can be approximated by the familiar Fox equation[23]:

$$\frac{1}{T_g} = \frac{w_1}{T_{g1}} + \frac{w_2}{T_{g2}}$$

where w_i represent the weight fractions and T_{gi} the glass transition temperatures for the polymers. A 50/50 wt % styrene–butadiene random copolymer, will have a glass transition temperature calculated on the basis of the Fox equation of approximately −14°C. If MAA is copolymerized with styrene and butadiene at a S/Bu/MAA ratio of 45/45/10, the calculated T_g would be −1°C, which is 25°C lower than that observed in the second-stage copolymers. Due to a different polymerization mechanism in the batch polymerization, with particle formation, as compared to the seeded polymerization there will be differences in the final polymer compositions resulting from the two methods even if the same monomer composition is used. In the batch experiments (R1 and R10), two fractions of polymer were present in both samples, because of a compositional drift in the polymer formed as the polymerization proceeds. A simulation of the batch terpolymerization[16] indicates that there will be one major polymer fraction having a T_g value associated with the low temperature transitions, observed as peaks in the tan δ curves in Figure 6 at 0°C for R1 and at 6°C for R10. Late in the polymerization a second polymer fraction rich in MAA and styrene will be formed, and this fraction will have a T_g higher than the first one. The second polymer fraction temperature transition can be observed in Figure 6 at 23 and 24°C, respectively for R1 and R10.

Samples C1 and C10 also showed a second transition at approximately 25°C, as indicated by an increase in the tan δ value for sample C1 (Fig. 7) and a weak shoulder for sample C10 (Fig. 8). The transitions may be related to a separate phase within the second-stage polymer. As seen in the TEM micrograph in Figure 1(e,f), a fraction of the second-stage polymer was present as small occlusions near or at the particle surfaces. Because of the high surface-to-volume ratio for this fraction, a high degree of grafting to PS can be anticipated, due to residual double bonds originating from the DVB used to crosslink the seed particles. This grafting would contribute to a higher T_g for this fraction. Furthermore, as with the unseeded batch copolymerizations, the compositional drift of the seeded copolymeri-

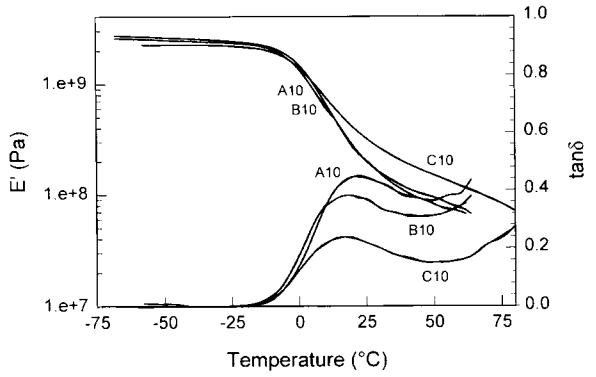

Figure 8 Storage modulus, E', and loss factor, tan δ, vs. temperature for films from samples A10, B10, and C10.

zation will lead to the formation of a polymer fraction richer in MAA and styrene, which would have a higher T_g than the copolymer formed earlier in the polymerization. Due to crosslinking and grafting, the small inclusions of the second-stage polymer in the seed particles should have a low tendency to migrate and, as seen in Figure 2(e,f), the small inclusions are still present in the seed particles after film formation. This fact indicates that the inclusions are immobilized and that they do not contribute to the properties of the rubbery matrix. The values of the storage modulus of these films indicate that the mechanical properties of the latex films were primarily dependent on the main phase domains of the second stage polymer, i.e., the larger occlusions seen in Figure 1(e,f). The two-phase structure of the second-stage polymer can also explain the poor film-forming ability of these latexes compared with the other latexes in the study.

It is obvious in Figures 7 and 8 that the samples prepared from the crosslinked PS seed (samples C1 and C10) show the highest values of the storage modulus in the rubbery region (0–50°C for C1 and 30–75°C for C10). These films contain irregularly shaped residues of the crosslinked seed particles, which seem to be interconnected by particle-to-particle contacts [Fig. 2(e,f)]. This may explain the high storage moduli observed, because the interconnected seed phase can take up load and can prevent the matrix polymer from deforming under stress. It is also clear in Figures 7 and 8 that the latex samples having a core–shell particle morphology (samples A10 and B10) have the lowest moduli in the rubbery region. The seed-particle residues in these films have an almost perfect spherical shape and they are evenly distributed in the second-stage polymer matrix without any particle-to-particle contacts. This is a clear indication that the core–shell morphology may not be the ideal one for attaining high moduli in the rubbery region in heterogeneous latexes having low film-forming temperatures.

CONCLUSIONS

The presence of a chain transfer agent reduced the glass transition of the second-stage copolymer containing 1 wt % MAA dramatically, whereas the rubbery plateau modulus was unaffected. When the MAA content was increased to 10 wt % the influence of the MAA monomer dominated on T_g, and all these latexes had similar T_g values, regardless of any chain transfer agent present in the second-stage polymerization.

Copolymerization of DVB with styrene in the preparation of the PS seed latexes substantially increased the rubbery moduli of the films, whereas the glass transition temperatures of the rubbery phase were unaffected. This could be explained by the effect of the latex particle morphology on the rubbery plateau modulus of the films. The presence of irregularly shaped seed particles in the film samples C1 and C10 had a considerable reinforcing effect on the films, due to particle-to-particle contacts. In contrast, the spherical seed particle fragments present in film samples A10 and B10, originating from latex particles having core–shell morphologies, did not contribute to the storage rubbery modulus. This fact strongly indicates that the ideal morphology for attaining low film-forming temperatures and a high modulus in the rubbery region for heterogeneous latexes may not be the core–shell morphology.

The authors from the Department of Chemical Engineering II at Lund University are grateful for the financial support for this work from MoDo AB and the Swedish National Board for Industrial and Technical Development, NUTEK. We should also like to thank Helen Hassander for the excellent electron microscopy work, Bodil Wesslén for her important assistance with the GPC analysis, and Dr. Anthony Bristow for the linguistic revision.

REFERENCES

1. R. Groves, J. E. Penson, and C. Ruggles, in *Tappi Proceedings of 1993 Coating Conference,* Tappi, Atlanta, 1993, pp. 187–193.
2. R. E. Hendershot and D. L. Meyers, in *Tappi Course Notes, 1994 Coating Binders Short Course,* Appleton, New York, 1994, pp. 59–70.
3. D. A. Kangas, *Coatings Plastics Preprints,* **36,** 353 (1976).

4. A. Zosel, W. Heckmann, G. Ley, and W. Mächtle, *Colloid Polym. Sci.*, **265,** 113 (1987).
5. T. Matsumoto, M. Okubo, and S. Shibao, *Kobunshi Ronbunshu, Eng. Ed.*, **5,** 784 (1976).
6. M. Okubo, Y. Katsuta, and T. Matsumoto, *J. Polym. Sci. Polym., Lett. Ed.*, **18,** 481 (1980).
7. M. Okubo, M. Ando, A. Yamada, Y. Katsuta, and T. Matsumoto, *J. Polym. Sci. Polym., Lett. Ed.*, **19,** 143 (1981).
8. M. Okubo, Y. Katsuta, and T. Matsumoto, *J. Polym. Sci. Polym., Lett. Ed.*, **20,** 45 (1982).
9. M. Okubo, K. Kanaida, and T. Matsumoto, *Colloid Polym. Sci.*, **265,** 876 (1987).
10. M. Okubo, Y. Murakami, and T. Youseke, *Chem. Express,* **8,** 253 (1993).
11. D. R. Stutman, A. Klein, M. S. El-Aasser, and J. W. Vandehoff, *Ind. Eng. Chem. Prod. Res. Dev.*, **24,** 404 (1985).
12. O. Karlsson, H. Hassander, and B. Wesslén, *J. Appl. Polym. Sci.*, to appear.
13. E. S. Daniels, M. S. El-Asser, A. Klein, and J. W. Vanderhoff, *Polym. Mater. Sci. Eng.*, **58,** 1104 (1988).
14. K. M. O'Connor and S.-L. Tsaur, *J. Appl. Polym. Sci.*, **33,** 2007 (1987).
15. M. Hidalgo, J. Y. Cavaille, J. Guillot, A. Guyot, C. Pichot, L. Rios, and R. Vassoille, *Colloid Polym. Sci.*, **270,** 1208 (1992).
16. O. Karlsson and B. Wesslén, work in progress.
17. O. Karlsson, H. Hassander, and B. Wesslén, *Colloid Polym. Sci.*, **273,** 496 (1995).
18. C. Winzor and D. C. Sundberg, *Polymer,* **33,** 3797 (1992).
19. J. Richard and J. Maquet, *Polymer,* **33,** 4164 (1992).
20. J. Y. Cavaille, R. Vassoille, G. Thollet, L. Rios, and C. Pichot, *Colloid Polym. Sci.*, **269,** 248 (1991).
21. R. E. Wetton, in *Development in Polymer Characterization,* J. V. Dawkins, Ed., Elsevier, Barking, 1986, Chap. 5.
22. J. Foreman, S. R. Sauerbrunn, and C. L. Marcozzi, in *Proceedings of 22nd NATAS Conference,* Denver, CO, 1993, pp. 55–58.
23. T. G. Fox, *Bull. Am. Phys. Soc.*, **1,** 123 (1956).

Received November 20, 1995
Accepted May 30, 1996